

LiDDA: Data Driven Attribution at LinkedIn

John Bencina*
LinkedIn Corporation
Sunnyvale, USA
jbencina@linkedin.com

Erkut Aykutlug*
LinkedIn Corporation
Sunnyvale, USA
eaykutlug@linkedin.com

Yue Chen
LinkedIn Corporation
Sunnyvale, USA
flchen@linkedin.com

Zerui Zhang
LinkedIn Corporation
Sunnyvale, USA
zerzhang@linkedin.com

Stephanie Sorenson
LinkedIn Corporation
Sunnyvale, USA
ssorenson@linkedin.com

Shao Tang
LinkedIn Corporation
Sunnyvale, USA
shatang@linkedin.com

Changshuai Wei†
LinkedIn Corporation
Seattle, USA
chawei@linkedin.com

Abstract

Data Driven Attribution, which assigns conversion credits to marketing interactions based on causal patterns learned from data, is the foundation of modern marketing intelligence and vital to any marketing businesses and advertising platform. In this paper, we introduce a unified transformer-based attribution approach that can handle member-level data, aggregate-level data, and integration of external macro factors. We detail the large scale implementation of the approach at LinkedIn, showcasing significant impact. We also share learning and insights that are broadly applicable to the marketing and ad tech fields.

CCS Concepts

• **Computing methodologies** → **Artificial intelligence**; • **Applied computing** → **Marketing**; • **Information systems** → **Online advertising**; • **Mathematics of computing** → *Probability and statistics*.

Keywords

Multi-Touch Attribution, Media Mix Modeling, Attention Mechanism, Computational Marketing, Deep Learning

1 Introduction

Marketers rely on attribution measurement to understand the impact of marketing campaigns on customers' journeys and decisions. Accurate attribution enables marketers to better optimize marketing spend and strategy to maximize their return on investment (ROI). In this paper, we propose a general framework for large scale end-to-end attribution system and details the implementation at LinkedIn, LiDDA. LiDDA leverages a combination of bottom-up and top-down modeling approaches in order to build a more accurate attribution platform to measure campaign performance and ROI. The system was originally developed for our internal Go-To-Market (GTM) marketing and has since expanded to support external applications for LinkedIn customers.

1.1 LinkedIn Use Case

GTM Marketing is responsible for managing digital marketing campaigns for various LinkedIn products (e.g., Recruiter Lite, Sales Navigator), targeting both acquisition and retention objectives, where audiences of marketing includes consumers and buyers. Consumer marketing focuses on the individual as a member such as member account signups. Buyer marketing focuses on the company-level conversions such as the use of LinkedIn Ads platform ads or Talent Solutions job posts.

Both segments are targeted using a combination of owned and external channels. Owned channels include Email and the LinkedIn Ads Platform (Feed Ads) where we own the platform used and have greater visibility to individual engagements. External channels refer to other online platforms such as Paid Search, Social Media, and Streaming. These channels do not provide individual level data, and we are often limited to aggregate information such as the total number of impressions in a time period.

One major challenge is lack of a unified view of the member journey across multiple channels. Existing media-mix-modeling (MMM) approaches provided channel-level visibility; however they could not provide more detailed campaign breakouts and journey information. Last touch attribution (LTA) was the default standard; yet it biased results to bottom of funnel (BOFU) campaigns and omitted channels without individual identifiers.

Through our work on LiDDA, we are able to build an approach which combines signals using both top-down and bottom-up information. This enables our marketing team to utilize attribution across different levels of granularity while still maintaining consistency. In the next section we further discuss the differences in top-down and bottom-up attribution approaches.

1.2 Overview of Related Work

Data-driven attribution (DDA) aims to measure the contribution of online campaigns at the user level using a bottom-up approach. On the other hand, Media-Mix modeling (MMM) considers both online and offline channels along with seasonality using a top-down (aggregate time-series) approach.

*These authors contributed equally

†Corresponding author

1.2.1 Media-Mix Modeling. Media mix models (MMM) uses aggregated time-series data to model conversions as a function of online and offline channels as well as macro-economic factors and seasonality. MMM have been widely used since the 1960s [3, 16], and provide a wholistic view across all channels and external factors. On the other hand, they come with different challenges [5]. One of the shortcomings is that they do not have visibility to analyze data at the user level.

1.2.2 Rules Based Attribution. Traditional attribution models uses rule-based attribution (RBA) approaches such as first-touch, last-touch, or time decay[9]. These approaches assign conversion credit based on simple, predetermined rules at user level. RBA methods are easy to understand and implement however, they are often based on limited assumptions and introduces biases.

1.2.3 Data-Driven Attribution. Data-driven attribution (DDA) addresses limitation of RBA by leveraging machine learning and statistical techniques to allocate conversion credit learned from Data. Different modeling approaches such as Logistic regression [18], Bayesian [1, 15] and Survival Theory [24] have been used. Deep learning approaches such as CAMTA [13], DNAMTA[14], and CausalMTA [23] have demonstrated improved performance with these classes of models.

1.3 Exploration on Existing Approaches

Ideally, credit is assigned according to its relative casual contribution. In practice, obtaining the ground-truth data for causal attribution is challenging. First, members are potentially exposed to dozens of overlapping treatments across different channels both on and off of our platform. Second, simulating realistic counterfactual journeys is further complicated by requiring touchpoint dimensions (eg. campaign metadata, timestamps) and the presence of sequential biases where subsequent engagements are influenced by prior interactions.

Given these challenges, we explored approaches to approximate the actual attribution for computational efficiency at scale. We first evaluated the Logistic Regression approach by Shao & Li [18]. Although straightforward, it requires making a separate prediction for every timestep in the sequence and using the change in outcome probabilities as credit. The model also lacks inherent ability to model sequences. We additionally observed a bias that early touches had larger incremental changes before plateauing as paths grew in length.

We also evaluated DNAMTA [14] which uses attention over LSTM however we found that the LSTM layer yielded end of path biases. This is likely because those hidden states had accumulated a greater amount of information useful for the classification task. We recognized that the use of transformer type of attention offered both single-pass inference and an explainability mechanism without requiring the LSTM component. Also, we realized that existing DDA models lacks consideration of missing data, whether from inherent availability gaps or privacy constraints, and do not adequately balance internal versus external channels or integrate with macro-level MMM frameworks.

1.4 Our contributions

As far as we know, LiDDA is the first industry deployed large scale DDA system that leverage transformer-type attention mechanism and can handle member-level, aggregate-level and integration of external macro factors. In particular, the system is highlighted by: (i) *Transformer Architecture*: our use of transformer type of attention offered both single-pass inference and an explainability mechanism; (ii) *Temporal-aware attention*: we discretize time gaps between campaign touchpoints and learn positional embeddings—plus a special day-of-week embedding—to capture both sequence order and seasonal effects; (iii) *Privacy-driven data imputation*: to correct for missing paid-media signals (e.g. due to GDPR/CCPA restrictions), we probabilistically inject aggregated impressions back into user paths; (iv) *Unified DDA&MMM outputs*: we reconcile discrepancies between independent DDA and macro-level MMM by scaling and aligning their channel attributions. (v) *End-to-end solution*: we present our modeling innovations, implementation details, comprehensive evaluation and insights from launching to both GTM marketing and Ads platform in the paper.

2 LiDDA System

2.1 System Overview

LinkedIn Data Driven Attribution (LiDDA) is our modeled attribution platform (Figure 1) which utilizes an attention-based modeling approach. Attention models are well suited for this task since they retain sequential information about the buyer journey and also enable us to incorporate additional features about the member, their company, and campaign information.

Overall, the model is structured as a binary classification task to predict whether a buyer journey will result in a conversion

$$P(C|E_M, E_C, S),$$

where C denote the binary conversion outcome, E_M denote the member embedding with length D_M , E_C denote the (member’s) company embedding with length D_C , and S denote the sequence of marketing touchpoints on the member with length N . E_M is a member embedding derived from LinkedIn data such as skills, titles, etc. that generally capture latent features of that member. Likewise, E_C is a company embedding derived from LinkedIn data such as industry, roles, etc.

From the trained model, we output the aggregated attention weight matrix from the touchpoint sequence S . The attention weights are normalized such that they add up to 1.0, i.e.,

$$\hat{\alpha}_i = \frac{\alpha_i}{\sum_{j=1}^n \alpha_j} \quad (1)$$

and the normalized weights are interpreted as percent contribution of that touchpoint to the final conversion event. We further discuss attention in Section 2.4.

The attention weights represent the relative credits within the path, however they still need to be rescaled for overall impact. We use a separate media-mix model (MMM) to adjust the MTA credits at the channel level to account for overall incrementality and channels where individual exposure data does not exist or is not available. This is discussed further in Section 2.7.

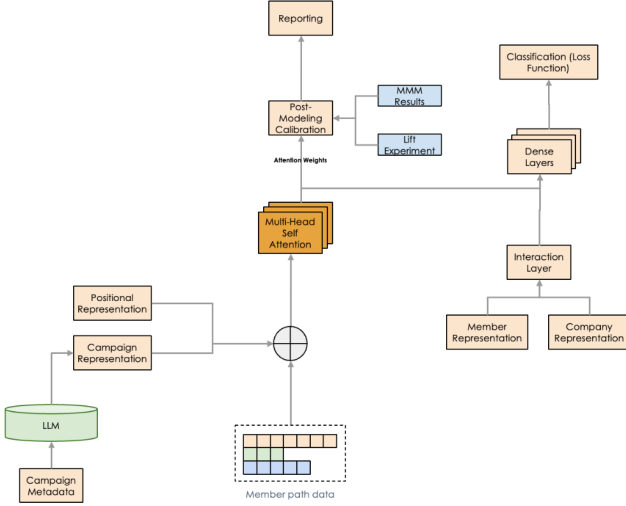


Figure 1: High level diagram showing the end-to-end components of our attribution modeling framework

2.2 Path Creation

2.2.1 Sequence Representation. The touchpoint sequence S is a time series of touchpoints $T \in \{t_0, \dots, t_{K+1}\}$ indexed by timestep t . K is the distinct number of possible (channel, action) pairs with 0 reserved for padding. An example of a (channel, action) could be (EMAIL, OPEN) or (AD, CLICK). The sequence S is limited to the last N touches such that paths with a length greater than N have their earliest engagements truncated. The choice of touchpoints included are context-specific and could represent marketing activities or other attributable steps in a defined journey.

During modeling, each touchpoint is represented as an integer and represented as a learned embedding E_T where $E_T \in \mathbb{R}^{T \times \text{dim}}$ which captures the latent information about the touchpoint. The embeddings are concatenated along the time dimension such that each path S is represented as a $N \times d$ tensor.

2.2.2 Touchpoint Representation. An additional feature, E_{MCID} , is concatenated to the learned E_T at each timestep. $E_{MCID} \in \mathbb{R}^{MCID \times \text{dim}}$ is an embedding representation of our marketing campaign which captures different aspects of the campaign such as its metadata or content. We obtain these embeddings from an upstream model which extracts a text description of the campaign and generates an embedded representation using an internal LLM fine-tuned on a LinkedIn corpus. This approach allows flexibility in combining structured and unstructured data consistently across domains.

2.2.3 Offline Processing. Our data pipeline process member events into marketing paths and augment the necessary features for modeling. We store these paths where they serve a dual purpose as model inputs and for use by marketing teams in post-modeling reporting. For model inference, we only define paths with respect to conversion events. The conversion event is the unique path identifier and anchor for all preceding touchpoints. During model training, we also generate a sample of non-converting paths with respect to the

current date to provide negative labels to our model. We utilize immutable conversion and touchpoint identifiers that allow downstream partner teams to easily connect attribution results to other data for further analysis and reporting.

2.3 Positional Representations

2.3.1 Positional Encodings. Attention models do not inherently model the order of touches in the paths so additional encodings are needed to capture the relative positions of each touch. Sinusoidal positional encodings are commonly used for temporal ordering as in the original attention design [21]. These are implemented as:

$$\begin{aligned} PE_{(pos, 2i)} &= \sin(pos/10000^{2i/d_{model}}) \\ PE_{(pos, 2i+1)} &= \cos(pos/10000^{2i/d_{model}}) \end{aligned} \quad (2)$$

Because our touchpoint embedding E_T is at the granularity of (channel, action), the number of possible combination is far lower than typical NLP vocabulary sizes. Therefore we use a substantially smaller embedding dimension for our data. We employ Time Absolute Position Encodings (tAPE) where the positional encoding definition in Equation (2) is modified to adjust for the lower dimensional representation[8]. The tAPE encodings are defined as:

$$\begin{aligned} \omega_k &= 10000^{-2k/d_{model}} \\ \omega_k^{new} &= \frac{\omega_k \times d_{model}}{L} \end{aligned} \quad (3)$$

2.3.2 Positional Embeddings. Positional encodings are not sufficient for our domain where marketing engagements are generated with irregular patterns and not across fixed intervals. For example, the time between an impression and the following click may be a few seconds while the time between two impressions could be days. We capture these irregular differences by representing the time difference between interactions as a discrete interval. For LinkedIn use cases, we use days as the interval unit since the look-back-window is limited to a few months based on business requirements.

Each touchpoint has a time interval relative to the final conversion state in the path, encoded by days as D with a corresponding learnt embedding E_D . Due to the strong seasonality of our marketing data, we also learn embeddings E_{DOW} corresponding to DOW encoding of each touchpoints.

We combine all the embeddings together for each touchpoint as:

$$\text{concat}(E_{MCID}, E_T) + E_D + E_{DOW} + \text{tAPE} \quad (4)$$

2.4 Attention Mechanism

We explored different methodologies for performing data driven attribution in our model as discussed in Section 1.2.3 and Section 1.3. In addition to their efficiency, models incorporating attention layers such as DNAMTA and CAMTA [13, 14], outperformed other model designs in this domain. Attention was originally proposed for NLP tasks [21], but later adopted in many other domains. Formally, attention is defined as:

$$\text{Attention}(Q, K, V) = \text{softmax}\left(\frac{QK^T}{\sqrt{d_k}}\right)V \quad (5)$$

We utilize the multi-head variation of attention where each head H has the ability to generate its own attention weights:

$$\text{MultiHead}(Q, K, V) = \text{Concat}(h_1, h_2, \dots, h_n) \quad (6)$$

The attention mechanism enables the model to adjust the weight given to different tokens in a sequence to optimally solve its objective. In LiDDA, we utilize a self-attention setup where Q , K , and V are equivalently the marketing engagements performed by the member. We apply attention over the sequence S and use the attention scores in the training classification task. The attention operation produces a representation of the sequence E_S where $E_S \in \mathbb{R}^{N \times H \times \text{dim}}$. We aggregate the heads by averaging the scores across the head dimension to obtain $E'_S \in \mathbb{R}^{N \times \text{dim}}$.

Different strategies exist for performing classification from attention scores. In BERT [6], the authors created a special [CLS] token at the start and use only the learned representation of the first token. Other valid approaches include max-pooling or mean-pooling over the entire sequence. During inference, we compute the final attribution output as the summation of the attention weights across all heads and then normalize each row to 1.0 such that each row represents a path and each value in that row represents the j -th touchpoint in that sequence. We set masked values to 0 if a path is shorter than our maximum length.

In LiDDA, we keep all attention scores by flattening the attention output. The motivation behind this decision is to retain as much positional information as possible when computing the attention weights. Additionally, we limit our attention module to a single layer in order to reduce behavior where attention interpretability may be affected by abstract representations across timesteps as discussed in the next section.

2.4.1 Attention for Attribution. Prior works [13, 14] utilize attention-based crediting by applying a self-attention layer over an recurrent network. Our initial exploration of this approach found a heavy bias towards end-of-path touches. Using a bi-directional LSTM may help alleviate this effect, however we modified the approach to directly apply self attention over the input sequence. One issue with the LSTM encoder is that the hidden state contains information about previous timesteps, making attention interpretation less straight forward [17]. The topic of attention interpretability has been the subject of extensive research [12, 22]. The central concern is that the resulting weights may not faithfully align with the model final output. While our modification can still introduce interpretability issues in attention based models [4], we observe within our domain that attention weights do impact model output. We share additional findings in Appendix A.1.

It is also possible to compute attribution based on the incremental propensity from the prior engagement [18] or as an approximation of Shapely values [23]. These methods are not necessarily superior. Counterfactual simulations can be computationally expensive and require accurately determining the counterfactual which is non-trivial. We did evaluate the attributions under the attention vs incremental propensity and found negligible differences (Table 1). We also observed that incremental propensity approach often produces early jumps causing front-loaded attribution as propensity gains saturate with length.

Channel	Incremental	Attention
Channel A	14.4%	12.7%
Channel B	52.3%	53.4%
Channel C	29.5%	32.5%
Channel D	3.8%	1.5%

Table 1: A LiDDA trained model was used to perform attribution under two methods. Incremental assigns attribution according to the incremental change in $P(C|T_i) - P(C|T_{i-1})$ while Attention uses only the attention weights.

2.5 Imputation of Paid Media Touchpoints

LinkedIn’s outbound marketing channels are grouped into owned and paid channels. When marketers use owned channels, Email and LinkedIn’s advertising platform, to market products and services to members, we can collect touchpoints from all actions at the user level, e.g., sends, opens, clicks, impressions. On the other hand, when external (paid) channels are used, due to privacy regulations like GDPR or CCPA, we cannot readily collect data at the user level (Figure 3).

When a member clicks on an ad on an external platform they land on a LinkedIn microsite. We can use the URLs from microsites as a proxy for paid clicks at the member level. On the other hand, we do not have any impression data at the member level. The lack of member-level impression data for paid media channels can bias attribution modeling.

While member-level data is not available for paid media channels, we can still obtain daily aggregate campaign-level data, e.g., number of impressions for a campaign on a given day, from external platforms. We leverage this aggregated data to mitigate the bias by imputing paid media impressions probabilistically. This is performed in two steps. First, we attach a certain number of impressions to existing click events, because each click necessarily must have prior impressions. Second, we look at how impressions are distributed across online members without any reference to clicks for each paid media channel. In both cases, we use owned channels as proxies to get prior information on these distributions, as shown in Figure 2.

One of the main challenges in leveraging multiple third-party platforms is that they report aggregate impressions for both members and non-members. On the other hand, DDA models only member data. Each 3rd party channel can have a different percentage of identifiable impressions. To this end, we estimate a downscaling factor for different 3rd party platforms using internal click-based based data to determine how many impressions should be distributed among members while modeling.

We analyze the distribution of how many impressions proceed each click event at the member level from owned channels. We also calculate the ratio of daily aggregate impressions to click from owned channels. Using these ratios, daily aggregate impression-to-clicks and the impressions-per-click at the member level, we infer how many impressions should be assigned to each click event for different paid-channels.

Using this prior information and daily impression-to-click ratio for each external paid channel, we assign impressions to existing

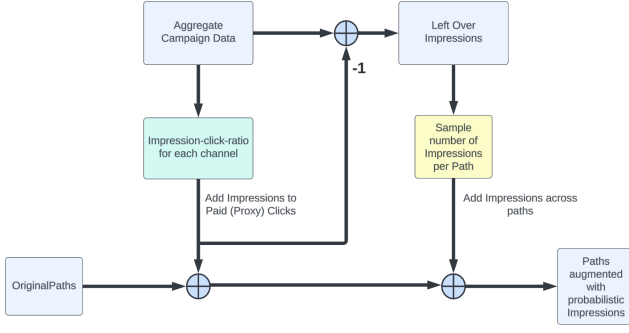


Figure 2: Probabilistic touchpoints are imputed in paths in two steps. First, we add impressions to existing proxy-click events based on impression to click ratio of each channel. Second, we distribute the remaining impressions across members online each day.

Algorithm 1 Paid Media Impression Imputation Methodology

Require: Member *touchpoint* data

Require: Aggregate external (paid) campaign *impression* data

$Imp_{AGG-campaign}$

for *touchpoint* **do**

if *touchpoint* is a click for paid – channel (*ch*) **then**

 Sample n pseudo impressions Imp_n from

$N(impratio_{ch}, \sigma^2)$

end if

end for

Compute total assigned pseudo impressions for each campaign:

$Imp_{campaign} = \sum_{paid-campaigns} Imp_n$

if $I_{AGG-remainder} = \sum(I_{AGG-campaign}) - Imp_{campaign} > 0$ **then**

 Sample N random members

for *member* **do**

 Sample $I_R \sim N(\mu, \sigma^2)$ random impressions

 Create touchpoint I_R until $\sum(I_R) = I_{AGG-remainder}$

end for

end if

paid proxy click events sampled from the distribution $N(impratio_{ch}, \sigma^2)$. Next, we distribute the remaining daily impressions from paid media campaigns across members randomly based on campaigns’ and members’ regions. While doing this, we apply an estimated member-to-nonmember ratio realizing that aggregated external impressions may belong to both members and non-members. We make sure the distributed impressions do not exceed the estimated limits. This methodology is summarized in Algorithm 1.

2.6 Sessionization & Downsampling

Another issue in modeling attribution is that certain channels have significantly more touchpoints compared to other channels in member paths due to signal bias. For example, emails may be sent once a week but in-feed ads could have multiple daily exposures. The

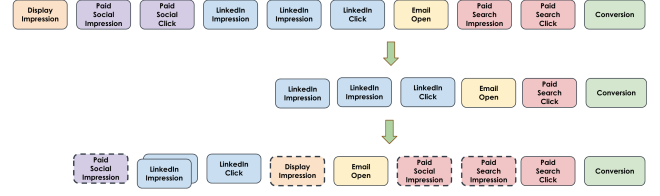


Figure 3: The top row shows an original path with all impressions and clicks a member has interacted with prior to making a conversion. We cannot collect any paid media impressions due to privacy regulations like GDPR and CCPA, and we use a fixed length for paths to use in modeling. The middle row shows the same path after these interactions are dropped. We impute probabilistic impressions into the paths and group impressions from owned channels, LinkedIn Platform as shown in the bottom row for modeling.

paths that go into attribution modeling are of fixed length, therefore touchpoints from owned channels may saturate the paths and reduce the representation of paid (external) touchpoints in paths. To make the representation of channels more balanced across paths, we perform two path adjustments which yield more balanced representations of engagements as shown in Figure 4.

Our attribution system is complex and heterogeneous, as a result, certain heuristic is necessary. Meanwhile, we perform comprehensive evaluation on these heuristics. For example, to downsample owned channel activities, we estimate a scaling factor to bring the number of actions, clicks/impressions, to the same order of magnitude of actions from other channels. And we evaluate the impact through offline and online experiment.



Figure 4: We group touchpoints from some owned channels, e.g., LinkedIn Platform, within a session into a single representative touchpoint. The attribution given to this one touchpoint is distributed evenly among the grouped campaigns.

2.6.1 Sessionization. First, we group impressions from certain channels in a path as a single touchpoint within a session if they are from the same campaign on the same day, as detailed in Algorithm 2. This helps reduce noise, particularly from on-platform channels where a member may observe the same campaign repeatedly due to scrolling behavior. With this approach, we model a single event however we retain the downsampling links for post-model processing to reallocate credit equally across the grouped events.

2.6.2 Downsampling. Secondly, we further address signal bias by adjusting the retention rate of specific channel, action combinations according to tunable downsampling rates. We obtain these rates using an independent analysis to estimate the comparable impact of each channel using signals such as spend and outcomes. With these ratios, we randomly drop some touchpoints to yield the

Algorithm 2 Sessionization methodology

Require: Member *path* with marketing *touchpoint* metadata

```

for path do
  Group all impressions by campaign, channel, and date
  for group do
    Select most recent touchpoint by timestamp
    Record array of remaining touchpoint
    Store array in touchpoint metadata
  end for
  Output truncated path with linkage metadata
end for

```

expected ratio as described in Algorithm 3. We observe that this pre-processing step yields more reliable attribution results and path compositions better aligned with aggregate data.

Algorithm 3 Downsampling methodology

Require: Member *path* with marketing *touchpoint* metadata

Require: Sampling *ratio* per *action* and *channel* pair

```

for path do
  Group all touchpoints by action and channel
  for group do
    Sort touchpoints by timestamp
    Compute number of touchpoints N based on ratio
    Retain N latest touchpoints
  end for
  Output truncated path
end for

```

2.7 Output Scaling

As we mentioned earlier, Media Mix Modeling (MMM) uses time-series (daily aggregated) data to model the contribution of seasonality as well as online (display, search, video, etc.) and offline (TV, direct mail, etc.) channels. On the other hand, Data-driven Attribution (DDA) models only online channels. Online channels being independently modeled by both MMM (top-down) and DDA (bottom-up) models can lead to inconsistent results for online channels. To provide marketers a unified view for each channel performance, we apply post-modeling calibration step where DDA predictions are aligned with those from MMM models.

MMM and MTA methodologies have been used in the industry for a long time. They are often used in silos without much connection. There has been some efforts lately to connect these top-down and bottom-up approaches [10], which models each online channel contribution as a regression on aggregate channels. Another approach could be to include any prior information as a constraint in modeling [7]. In this work, we take a different approach of scaling MTA results in post-modeling to match attribution results from MMM at the channel-level or at a different granularity.

We combine signals from our top-down MMM model with our bottom-up DDA model to create a single attribution view for the marketer. We utilize MMM to perform channel-level attribution and measure marketing incrementality in the context of macroeconomic

factors, however it cannot measure specific member journeys. Conversely, DDA can perform attribution on specific interactions, but has some signal limitations. Specifically where we are unable to collect individual-level signals due to privacy restrictions or inherent channel limitations (ie. radio, events, television). Two independent attribution systems may not converge to the same point of view, particularly if they utilize different interactions. We address this by performing a post-modeling scaling across both DDA and MMM. This enables consistency at the top-level while allowing for more granular attribution within each channel to specific campaigns or engagements.

In post-modeling calibration we multiply the attribution of each touchpoint in a channel by the ratio of total number of attributed conversions by MMM to those by DDA in each channel. This does not change the relative relationship between the attribution of touchpoints from campaigns within that channel group predicted by DDA.

3 Experimental Validation and Calibration

The goal of the attribution model is to proportionally quantify the impact of each marketing action towards a conversion. Since there is no ground-truth data on the contribution of each action towards a conversion, we perform the following offline and online validations to evaluate the attribution model's predictions.

3.1 Offline Validation

In offline validation, we seek ensure the model's accuracy and stability as these are intuitively desirable properties of any attribution system. Because our offline process only has access to observational data, we primarily focus on typical ML performance as guardrails rather than actual attribution accuracy, as we discuss in Section 3.2.

3.1.1 Training Stability. We first assess the model's performance using binary classification metrics, aiming for high predictive accuracy (validation ROC-AUC & PR-AUC > 0.9 before calibration). To test the model's sensitivity to training data, we retrain the attribution model on 10 subsets of the training data and evaluate them on the same hold out dataset. The 10 resulting models' performance (Figure 5) and predicted action weights (Figure 6) converge, confirming that the model exhibits consistent results.

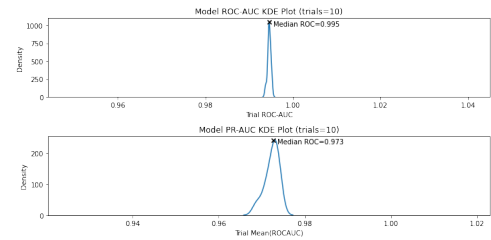


Figure 5: The distribution of ROC-AUC and PR-AUC of models retrained on 10 different subsets of training data and measured against a constant holdout. These models performance metrics converge.

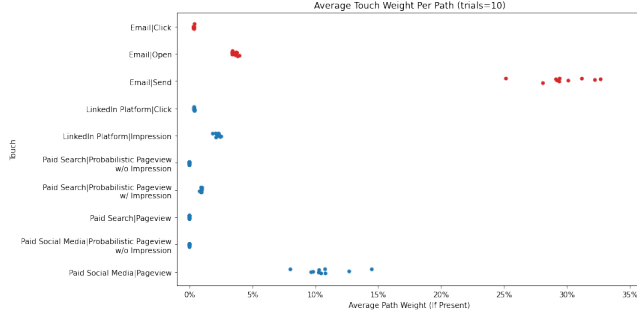


Figure 6: The weight (x-axis) assigned to different actions (y-axis) in models retrained on 10 different subsets of training data (dots).

3.1.2 Inference Stability. We perform a similar check on our model’s stability on inference data. For each action, we bootstrap sample the action’s weights with replacement for 100 times, calculate the average, and then analyze the distribution of the 100 averages to evaluate the stability of the predicted weights (Figure 6). We observe that the weights of each action converge. While this approach does not have an intrinsic absolute threshold, we use these values as guardrails across runs to monitor for potential issues.

Lastly, we evaluate the stability of the conversion propensities over time, using the Anderson-Darling statistic [2, 19] on our data to evaluate whether the conversion propensities each day are from same distribution as those a week ago. We assume that the general distribution of conversion propensities should be roughly equivalent in a short period of time. The result shows that the conversion propensities each day are mostly from the same distribution.

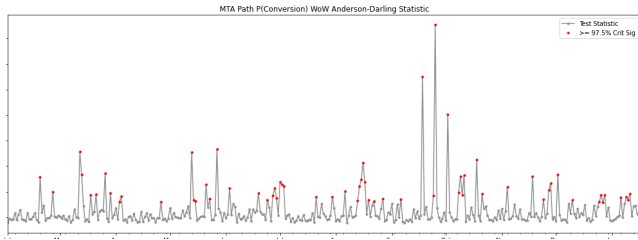


Figure 7: Anderson-Darling statistic comparing the conversion propensities each day to those a week ago. Days where the propensities are significantly different are marked in red.

3.2 Online Validation

Offline validation does not give us insight into whether the predicted interaction weights are close to actual member behaviors. Thus, we run experiments as online validations, in which we measure the incremental effect selected campaigns have on conversions and compare it with our model predicted lift. These experiments allow us to check how close our attribution model’s predicted interaction weights align with real-world marketing efforts. We can run member-level incremental lift tests for owned channels (email and

the LinkedIn platform), but we can only run geo-level experiments for external paid channels (Google Ads, Facebook, etc).

For the owned channels including email and the LinkedIn platform, we randomly split members into two groups. We select certain campaigns to hold out email sending during the experiment in the control group and conduct business as usual in the treatment group. We calculate the combined lift of the campaigns from the conversion rates of the treatment and control group. It is important to note that email sending was sparse across both members and time, limited to approximately one email per week to a small set of selected members within the connection graph. Additionally, AA tests were conducted as a basic validation of the experimental setup, and no statistically significant differences in conversion rates were found between groups, suggesting that network effects did not contaminate the results.

To validate member-level experiment, we simulate a holdout experiment within the treatment group by creating counterfactual conversion paths, where the holdout campaign touchpoints are omitted. This approach helps estimate what the conversion path would look like had the member been in the control group. This counterfactual path is a simulation of the member’s path if the customer is in the control group under two assumptions based on the experiment setup validation above: 1) members’ interaction with other campaigns were not affected by the holdout 2) members did not receive extra campaigns in place of the holdout. We use the attribution model to generate two modeled conversion probabilities:

- $P(\text{Conversion})$: Original path probability
- $P'(\text{Conversion})$: Counterfactual path probability

We then define the lift calculation for the holdout campaign as:

$$\text{Lift} = \frac{P'(\text{Conversion})}{P(\text{Conversion})} - 1 \quad (7)$$

We compare the distribution of this simulated lift of all conversion paths against the confidence interval of the measured lift.

3.3 Calibration

There are several challenges during the experimental validation. First, the simulation of counterfactual paths by adding touches requires more assumptions such as sequencing and campaigns which may introduce noise. Second, due to the scale of our interaction data, we also do not retain the journey paths from non-converted members which complicates the measurement of control groups in model prediction. Third, the simulation can therefore only depend on the observed paths from the converted members in the treatment group which is a biased representation of outcomes for general online experiments with randomized control and treatment groups.

To mitigate the gap for selection bias in the third challenge, we fit a propensity score model for the subset of converted members in the treatment group based on the member embeddings and their group assignment, and then adjust the conversions in the test period by the inverse propensity score weighting (IPW) [11]. Denote e_i as the propensity score for member i and Z_i as the indicator for member i receiving campaigns as in the treatment group ($=1$) and for being in the control group ($=0$). Denote E_{M_i} as the member embeddings for member i that is computed by LinkedIn.

Step 1: Estimate each member's conversion propensity

$$e_i = P(Z_i = 1 | E_{M_i}) \quad (8)$$

Step 2: Compute the IPW

$$w_i = \begin{cases} 1, & \text{if } Z_i = 1 \\ \frac{e_i}{1-e_i}, & \text{if } Z_i = 0 \end{cases} \quad (9)$$

This inverse propensity score weight can help balance the converted members in the treatment group and members in control group for fairer comparison between model predicted conversions and observed conversions from online experiments. In Figure 8, we create weight-scaled pseudo-populations through $1/w_i$ for those who converted in the treatment group and for those in the control group. We observe that IPW functions as expected to adjust the population from converted member in treatment group and control group to a closer match. In the next section, we apply the simulation and IPW adjustment to an online experiment result.

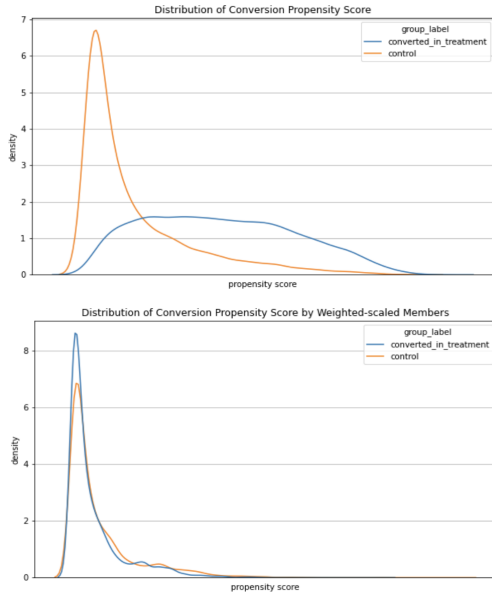


Figure 8: The top chart shows a mismatch between conversion propensity score distribution for converted members in the treatment group vs. control members. The bottom chart shows that conversion propensity score distributions are better matched in the pseudo-populations where we replicate the members through $1/w_i$ to balance the two populations.

3.4 Experiment Results

We chose three incrementality tests in the email channel to validate the attribution model and the primary metric is conversion lift defined in 7. Our goal is to evaluate the effectiveness of the acquisition email series. The workflow is illustrated in Figure 9 and the comparisons are listed in Table 2.

Confidence intervals for the experimental observations were derived using the delta method [20], and confidence intervals for the adjusted and simulated results were derived using a bootstrap

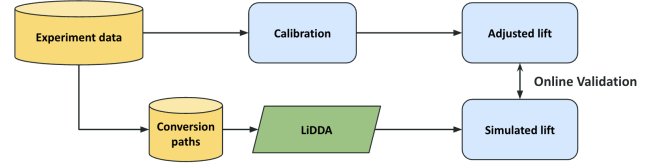


Figure 9: The online validation refers to the comparison between measured lift from experiment data and the simulated lift output by LiDDA and the aforementioned calibration

Test index	Experimental	Adjusted	Simulated
1	6.67% (-2.68%, 16.02%)	9.74% (-0.66%, 20.14%)	12.54% (10.52%, 14.73%)
2	9.73% (1.71%, 17.75%)	14.05% (3.35%, 24.75%)	19.61% (16.81%, 23.44%)
3	16.65% (3.93%, 29.37%)	12.46% (-3.52%, 28.44%)	9.54% (7.53%, 11.75%)

Table 2: Experimental validation for 3 incrementality tests. Each cell contains the mean lift and its corresponding 95% confidence intervals. The confidence intervals in the first column are derived from delta method and those in the second and third columns are derived from bootstraps.

with 1000 replicates. We notice that the gaps between experimental conversion lift and the simulated conversion lift were mitigated by applying the inverse propensity score weighting, and Z-score showed that adjusted conversion lift had no significant deviation from the simulated conversion lift. We concluded that our result directionally align with the experimental results.

4 Application to LinkedIn Ads Measurement

The LiDDA model architecture was first applied to LinkedIn's GTM marketing. We have since integrated a variant of LiDDA into LinkedIn's Ad Platform to provide advertisers with comprehensive funnel insights through LinkedIn Ads. Previously, measurement of ad impact on the Ads platform heavily relied on last-touch attribution, which often undervalues upper-funnel ads, potentially resulting in suboptimal budget allocation. In contrast, data-driven attribution distributes credit across multiple ad interactions throughout the buyer's journey, accounting for the impact of upper-funnel advertising efforts on business outcomes.

When applying LiDDA to the LinkedIn Ads use case, we also supply information about the advertiser, via a company embedding for the advertiser. This is concatenated with embeddings representing the member and their company. Similar to our GTM marketing model, we also include a touchpoint sequence representation (encoding the sequence of touch types, e.g., "Onsite lead generation sponsored status update video ad impression"), touchpoint embeddings derived from campaign text, and positional encodings (representing the time between each touchpoint and the conversion). While GTM marketing has access to touchpoints across multiple channels, the Ads platform currently only has access to LinkedIn touchpoints. When applying the model to lead conversions obtained through LinkedIn's Lead Generation form, on average the attribution weights show a time decay effect: touches closer to the conversion tend to get more credit (Figure 10).

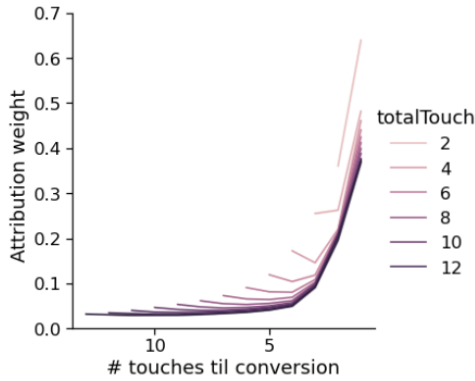


Figure 10: Attribution weights for LinkedIn lead conversions show a time decay effect in aggregate; ad touches closer to the conversion tend to get more credit (i.e., higher attribution weights). Note: the attribution weights for a given conversion will always sum to one.

Meanwhile, touchpoint-level attribution from LiDDA provides very granular insights, where we see varying credit assignment to earlier touchpoints. In the provided examples in Figure 11, touches closer to the conversion tend to have higher weights; however, the weight assigned to a specific touchpoint can vary, influenced by factors like the objective type, ad format, interaction type (impression, click), ad creative, days before conversion, etc. Using these types of signals, the model can learn to allocate credit across all touchpoints in the converting paths. This data can then be surfaced to advertisers on LinkedIn’s Ad platform at different levels of aggregation, in a variety of ways, including in the Campaign Manager Reporting table (i.e., showing the number of conversions attributed to each campaign, creative, etc.), and in a plot in Measurement Insights (showing a time series of conversions attributed to different categories of campaigns).

5 Conclusion

In this paper, we introduce LiDDA, a unified transformer-based data-driven attribution approach we developed and deployed at LinkedIn. We demonstrated the innovations to DDA methodology that combines an attention mechanism, positional embeddings, touchpoint imputation, sessionization, and MMM. We also shared learnings from implementation and deployment that are broadly applicable to the Marketing and Ad tech fields.

References

- [1] P.K. Kannan A. Li. 2014. Attributing Conversions in a Multichannel Online Marketing Environment: An Empirical Model and a Field Experiment. 51:40-56, 02 pages.
- [2] T. W. Anderson and D. A. Darling. 1952. Asymptotic Theory of Certain 'Goodness of Fit' Criteria Based on Stochastic Processes. *The Annals of Mathematical Statistics* 23, 2 (1952), 193–212. <http://www.jstor.org/stable/2236446>
- [3] N.H. Borden. 1964. The Concept of the Marketing. 4, 2-7 pages.
- [4] Gino Brunner, Yang Liu, Damian Pascual, Oliver Richter, Massimiliano Ciaranita, and Roger Wattenhofer. 2020. On Identifiability in Transformers. In *8th International Conference on Learning Representations (ICLR 2020)(virtual)*. International Conference on Learning Representations.
- [5] David Chan and Mike Perry. 2017. *Challenges and Opportunities in Media Mix Modeling*. Technical Report.

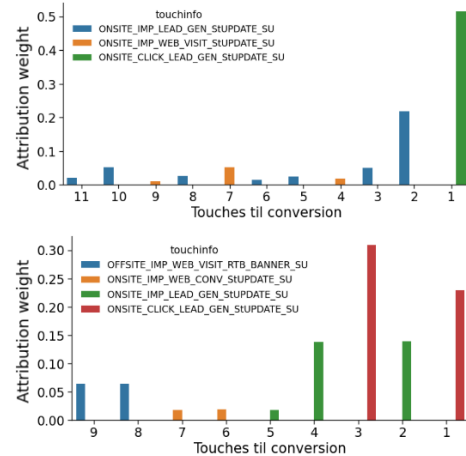


Figure 11: The attribution weights extracted from the model can provide granular insights. Here we show example attribution weights for two LinkedIn lead conversions, as a function of touches until conversion (x-axis) and touch type (hue). While in aggregate we see a time-decay effect (i.e., touches closer to the conversion tend to get more credit), the credit allocated to each touch in a given path can vary. For example, in the bottom path, the initial blue touches receive relatively more credit than the next few touches, and the red "click" three touches before the conversion receives the highest credit.

- [6] Jacob Devlin, Ming-Wei Chang, Kenton Lee, and Kristina Toutanova. 2019. BERT: Pre-training of Deep Bidirectional Transformers for Language Understanding. arXiv:1810.04805 [cs.CL] <https://arxiv.org/abs/1810.04805>
- [7] Facebook Experimental. [n. d.]. Robyn. <https://facebookexperimental.github.io/Robyn/>
- [8] Navid Mohammadi Foumani, Chang Wei Tan, Geoffrey I. Webb, and Mahsa Salehi. 2023. Improving position encoding of transformers for multivariate time series classification. *Data Mining and Knowledge Discovery* 38, 1 (Sept. 2023), 22–48. doi:10.1007/s10618-023-00948-2
- [9] Jitendra Gaur and Kumkum Bharti. 2020. Attribution modelling in marketing: Literature review and research agenda. *Academy of Marketing Studies Journal* 24, 4 (2020), 1–21.
- [10] Google. [n. d.]. Unified Marketing Measurement. The Power of Blending Methodologies. https://www.thinkwithgoogle.com/_qs/documents/15401/UnifiedMarketingMeasurement.pdf
- [11] Miguel A Hernán and James M Robins. 2006. Estimating causal effects from epidemiological data. *Journal of Epidemiology & Community Health* 60, 7 (2006), 578–586.
- [12] Sarthak Jain and Byron C. Wallace. 2019. Attention is not Explanation. In *Proceedings of the 2019 Conference of the North American Chapter of the Association for Computational Linguistics: Human Language Technologies, Volume 1 (Long and Short Papers)*, Jill Burstein, Christy Doran, and Tamar Solorio (Eds.). Association for Computational Linguistics, Minneapolis, Minnesota, 3543–3556.
- [13] Sachin Kumar, Garima Gupta, Ranjitha Prasad, Arnab Chatterjee, Lovekesh Vig, and Gautam Shroff. 2020. Camta: Causal attention model for multi-touch attribution. In *2020 International Conference on Data Mining Workshops (ICDMW)*. IEEE, 79–86.
- [14] Ning li, Sai Kumar Arava, Chen Dong, Zhenyu Yan, and Abhishek Pani. 2018. Deep Neural Net with Attention for Multi-channel Multi-touch Attribution. arXiv:1809.02230 [cs.LG] <https://arxiv.org/abs/1809.02230>
- [15] Andrew Whinston Lizhen Xu, Jason A. Duan. 2014. Path to Purchase: A mutually exciting point process model for online advertising and conversion. 60(6):1392-1412 pages.
- [16] J. E. McCarthy. 1978. Basic marketing: a managerial approach.
- [17] Sofia Serrano and Noah A Smith. 2019. Is Attention Interpretable?. In *Proceedings of the 57th Annual Meeting of the Association for Computational Linguistics*. 2931–2951.

- [18] Xuhui Shao and Lexin Li. 2011. Data-driven multi-touch attribution models. In *Proceedings of the 17th ACM SIGKDD international conference on Knowledge discovery and data mining*. 258–264.
- [19] M. A. Stephens. 1974. EDF Statistics for Goodness of Fit and Some Comparisons. *J. Amer. Statist. Assoc.* 69, 347 (1974), 730–737. doi:10.2307/2286009
- [20] Aad W. van der Vaart and Jon A. Wellner. 1996. *The Delta-Method*. Springer New York, New York, NY, 372–400. doi:10.1007/978-1-4757-2545-2_35
- [21] Ashish Vaswani, Noam Shazeer, Niki Parmar, Jakob Uszkoreit, Llion Jones, Aidan N. Gomez, Lukasz Kaiser, and Illia Polosukhin. 2017. Attention is all you need. *Advances in Neural Information Processing Systems* (2017).
- [22] Sarah Wiegrefe and Yuval Pinter. 2019. Attention is not not Explanation. In *Proceedings of the 2019 Conference on Empirical Methods in Natural Language Processing and the 9th International Joint Conference on Natural Language Processing (EMNLP-IJCNLP)*. 11–20.
- [23] Di Yao, Chang Gong, Lei Zhang, Sheng Chen, and Jingping Bi. 2022. Causalmta: Eliminating the user confounding bias for causal multi-touch attribution. In *Proceedings of the 28th ACM SIGKDD Conference on Knowledge Discovery and Data Mining*. 4342–4352.
- [24] Ya Zhang, Yi Wei, and Jianbiao Ren. 2014. Multi-touch attribution in online advertising with survival theory. In *2014 IEEE International Conference on Data Mining*. IEEE, 687–696.

A Additional Offline Analysis

A.1 Attention Interpretability

When using attention weights in attribution, we would expect that the computed weights quantify the contribution a touchpoint has towards the prediction of a conversion outcome. Therefore, if we were to modify the weight distribution we should observe a change in the predicted outcome. In this test, we train two models on the same dataset. The baseline model is trained using the standard attention setup described in this paper. The modified model randomly permutes the attention weights at a path-level during inference forward passes.

We train both models for 10 epochs each using identical batch sizes and hyperparameters. After training, we perform an inference pass on a shared holdout dataset and measure ROC-AUC. For the baseline model, we perform a single inference pass. For the modified model, we perform 10 inference passes to capture the variance introduced by the weight permutation process. We repeat this entire process 30 times for each model.

In Figure 12, we observe that the baseline model generally yields higher performance with a median ROC-AUC of 0.956 while the modified model has a median ROC-AUC value of 0.928 (−2.93%). While this is not a substantial change, we observe a larger negative impact on the consistency of results. The AUCs of both models are noted to be high. There are two explanations for this. One reason is due to resampling of the data creating an artificially high rate of conversions. The model is measured on uncalibrated results. Secondly, we note that in our domain, converting paths have a notably different composition which facilitates an easier classification task.

In Figure 13, we plot the results of the 30 modified trials sorted in median ascending order. 23 of the 30 trials ranked below the 20th percentile compared to the baseline model. We conclude from this test that the introduction of weight noise has a material impact on model performance and therefore provides some explainability power.

A.2 Ablation

A.2.1 Methodology. We performed an ablation study to estimate the contribution of different components of our model introduced in this paper. We generated fixed training, validation, and inference

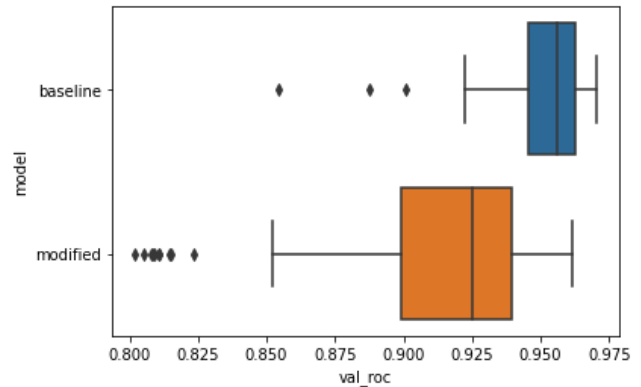


Figure 12: The plot compares the ROC-AUC against a common holdout for both the baseline and modified attention models in our study. The baseline model consists of 30 datapoints with 1 validation step per trial. The modified model consists of 300 datapoints with 10 validation steps per trial.

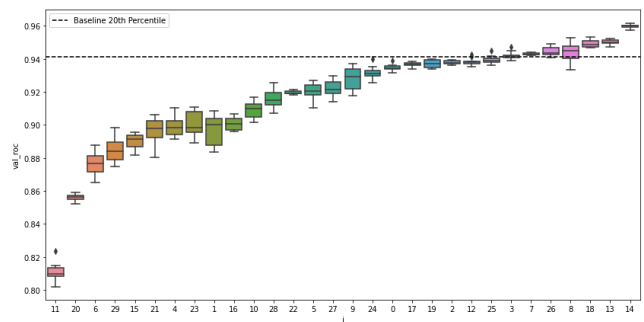


Figure 13: This plot shows the per-trial results for the modified model. The trials are sorted in ascending order according to their median ROC-AUC value. We observe that 23 of the 30 models fall below the bottom 20th percentile of the baseline trials.

datasets to use across each simulation where a new model was trained and inferred with the indicated component removed. In each simulation, the removal of the component was performed by modifying the code to omit the component from the graph. All hyperparameters and were held constant, and each model was trained for 5 epochs.

After training, we evaluated the ROC-AUC metrics against the validation dataset which contains a resampled population ratio of non-converting to converting of 10:1. We also evaluated the attribution weight distribution across channels for each of the models.

We tested the following components of the model:

- **Baseline:** The unmodified model as described in the paper
- **No-Entity:** Member and company embedding inputs removed
- **No-Campaign:** Touchpoint campaign embedding inputs removed
- **No-Date:** Touchpoint date embedding inputs removed

- **Seq-Only:** All embeddings removed leaving only the sequence and positional encoding

A.2.2 Classification Results. We first evaluated the ablation effects on the final classification power of the model by comparing the predicted model score to . We note high nominal AUC values as the simulations were performed on a resampled dataset. We observe that there is a moderate performance loss for the touchpoint level date and campaign features. Removal of entity embeddings had a larger effect, and removal of all components had the most negative effect. We also note that utilizing the sequence only allows for substantial predictive power given that converting members in our domain behave differently than non-converting members.

Version	ROC-AUC	% Change
1. Baseline	0.990	–
2. No-Campaign	0.989	-0.1%
3. No-Date	0.984	-0.3%
4. No-Entity	0.973	-1.7%
5. Seq-Only	0.939	-5.1%

Table 3: ROC-AUC performance measured on a constant validation dataset after 5 epochs of training. Percentage change vs. the baseline model is shown.

A.2.3 Weight Results. We next evaluated the impact of the component removal on the measured attribution credit across a grouping of our four marketing channel families. We compute the the mean squared deviation in total attribution from the baseline model across the four channels as a measure of volatility in the ablation. We observe that all ablations result in some changes to attribution however removing the dates alone causes the most significant shifts.

Version	Mean Squared Deviation
1. Baseline	–
2. No-Campaign	8.5
3. No-Date	49.3
4. No-Entity	14.4
5. Seq-Only	11.8

Table 4: The percent attribution allocated across four marketing channels is computed using the indicated LiDDA model version. The absolute deviation for each channel vs. the baseline model is computed. The reported number is the mean squared deviation for that model, across all channels, compared with the original baseline mix.